Similarities and differences between myocarditis following COVID-19 mRNA vaccine and multiple inflammatory syndrome with cardiac involvement in children

Donato Amodio [a,b], Giuseppe Rubens Pascucci [a,b], Nicola Cotugno [a,b], Chiara Rossetti [a], Emma Concetta Manno [a], Chiara Pighi [a], Elena Morrocchi [a], Annamaria D'Alessandro [c], Marco Alfonso Perrone [d,e], Alessandra Valentini [f], Alessio Franceschini [d], Marcello Chinali [d], Annalisa Deodati [b,g], Chiara Azzari [h], Paolo Rossi [a,b], Stefano Cianfarani [b,g,i], Marco Andreani [j], Ottavia Porzio [c,k], Paolo Palma [a,b,*]

[a] Research Unit of Clinical Immunology and Vaccinology, Bambino Gesù Children's Hospital, Istituto di Ricovero e Cura a Carattere Scientifico (IRCCS), Rome, Italy
[b] Department of Systems Medicine, University of Rome "Tor Vergata", Rome, Italy
[c] Clinical Biochemistry Laboratory, IRCCS "Bambino Gesù" Children's Hospital, 00165 Rome, Italy
[d] Department of Medical and Surgical Cardiology, Bambino Gesù Children's Hospital, IRCCS, 00165 Rome, Italy
[e] Division of Cardiology and CardioLab, Department of Biomedicine and Prevention, University of Rome Tor Vergata, Italy
[f] Department of laboratory Medicine, University Hospital "Tor Vergata", Rome, Italy
[g] Diabetology and Growth Disorders Unit, Bambino Gesù Children's Hospital, IRCCS, 00164 Rome, Italy
[h] Department of Health Sciences, Section of Pediatrics, University of Florence, Florence, Italy
[i] Department of Women's and Children's Health, Karolinska Institutet, 17177 Stockholm, Sweden
[j] Transplantation Immunogenetics Laboratory, Bambino Gesù Children's Hospital, IRCCS, Rome, Italy
[k] Department of Experimental Medicine, University of Rome 'Tor Vergata', Rome, Italy

ARTICLE INFO

ABSTRACT

Despite the multiple benefits of vaccination, cardiac adverse Events Following COVID-19 Immunization (c-AEFI) have been reported. These events as well as the severe cardiac involvement reported in Multisystem inflammatory syndrome in children (MIS-C) appear more frequent in young adult males. Herein, we firstly report on the inflammatory profiles of patients experiencing c-AEFI in comparison with age, pubertal age and gender matched MIS-C with cardiac involvement. Proteins related to systemic inflammation were found higher in MIS-C compared to c-AEFI, whereas a higher level in proteins related to myocardial injury was found in c-AEFI. In addition, higher levels of DHEAS, DHEA, and cortisone were found in c-AEFI which persisted at follow-up. No anti-heart muscle and anti-endothelial cell antibodies have been detected. Overall current comparative data showed a distinct inflammatory and androgens profile in c-AEFI patients which results to be well restricted on heart and to persist months after the acute event.

1. Introduction

Cardiac involvement represents a serious complication of SARS-CoV-2 infection that can occur during the acute phase of the disease but can also represent a hallmark of the multisystem inflammatory syndrome in children (MIS-C). SARS-CoV-2 vaccines have proven to be the most powerful approach for curbing the COVID-19 pandemic and to avoid severe infectious complications. Although the benefits of COVID-19 vaccination largely outweigh the risks, rare serious adverse events have been reported [1,2].

Among these, myocarditis after vaccinations represent a rare but scary adverse event [3,4]. Between 1990 and 2018, Centers for Disease Control and Prevention (CDC) and Food and Drug Administration (FDA) reported myopericarditis as 0,1% of all vaccine adverse events [5].

In July 2021, the CDC identified an association between the two licensed COVID-19 mRNA vaccines and myocarditis and pericarditis [6].

Patients identified by the Vaccine Adverse Event Reporting System (VAERS) were categorized according to CDC work case definitions as probable myocarditis, confirmed myocarditis, or acute pericarditis [6,7].

To date, according to the CDC VAERS [8], through July 11th, 2023, 691 possible myocarditis/pericarditis cases have been reported after COVID-19 mRNA vaccination in the U.S.A. The global incidence of myocarditis after COVID-19 mRNA vaccine seems to be low, estimated as 0.3–5.0 cases per 100,000 vaccinated people in case series studies from the U.S.A. and Israel [9–12].

The updates indicated that the risk of myocarditis or pericarditis after COVID-19 mRNA vaccination is higher among men aged 18–29 years, especially after the second dose [10–15]. The risk is increased 7 days following both vaccines [16]. The risk of acute myocarditis associated with COVID-19 mRNA vaccination has garnered intense attention although infrequent and usually resolving within days or weeks [13,17]. Since SARS-CoV-2 shows a specific heart tropism and given its ability to induce inflammation mostly in young adult male [18,19], we analyzed clinical and routine laboratory data along with androgens levels and high-dimensional proteomic analysis in a cohort of pediatric patients developing myocarditis following mRNA COVID-19 vaccination (c-AEFI), in comparison with age matched groups of patients with MIS-C, SARS-CoV-2 infected patients with few/moderate symptoms not requiring intensive care (CoV-2+) and healthy controls (HC).

2. Methods

2.1. Study participants and study design

This prospective observational study included pediatric patients referring to the Emergency Department of the Bambino Gesù Children Hospital for cardiac events (suspected acute myocarditis/pericarditis) after mRNA based COVID-19 vaccines [20].

A local ethical committee approved the study and written informed consent was obtained from all participants or legal guardians.

Clinical data were collected (Table. 1 and Supplementary Table S1). All patients were hospitalized and subjected to sample on admission or within 48 h for baseline evaluation, and within 6 months for follow-up evaluation (Fig. 1A-B). Cardiological evaluation with electrocardiogram (ECG) and echocardiogram were also performed.

Among the patients observed due to chest pain after COVID-19 mRNA vaccine (BNT162b2 mRNA-Pfizer-BioNTech and the mRNA-1273-Moderna), from August 2021 to February 2022, we enrolled 17 patients with CDC work case definitions for myocarditis [21]. One patient was ruled out because he was taking a potentially cardiotoxic drug (Dasatinib, a tyrosine kinase inhibitor) and one patient was excluded because she presented a history of idiopathic recurrent serositis from 2012.

Clinical cases have been categorized according to CDC work case definitions as probable myocarditis, confirmed myocarditis, or acute pericarditis [6,22–24] here referred to as c-AEFI. A group of these patients have been previously described [20].

Thanks to the CACTUS study [25–27], we could benefit from a previous cohort consisting of children affected by SARS-CoV-2 infection; children with MIS-C with cardiac involvement and before any treatment; healthy children collected in the pre-pandemic era. To avoid the potential confounding factor of age, we selected age matched patients and used for comparison of proteomic analysis 21 children with acute SARS-CoV-2 infection (CoV-2+), 14 children with MIS-C and 31 HC (Fig. 1A). Finally, we compared androgen levels in children with myopericarditis after mRNA vaccination (15 patients), MIS-C (13), CoV-2+ (9) and HC (22).

2.2. Proteomic assay

Plasma proteins were analyzed using a multiplex technology based upon proximity-extension assays [28] as previously described [25–27]. We measured specific proteins using the Olink® panel of Inflammation. Briefly, the kit consisted of a microtiter plate for measuring 92 protein biomarkers in 88 samples and each well contained 96 pairs of DNA-labeled antibody probes

The pre-processed data were reported in arbitrary units as Normalized Protein Expression (NPX) that enables individual protein analysis across a sample set analyzed in log2 scale, wherein a higher NPX correlates with higher protein expression. The data were pre-processed using the NPX Manager Software and OlinkAnalyze R package (version 1.3.0).

Table 1
Clinical and routine laboratory characteristics of the study groups.

	c-AEFI	MIS-C	CoV-2+	HC	p-value
Gender (F:M)	02:13	03:11	10:11	09:22	$p = 0.0399$ (c-AEFI vs CoV-2+)
Age (years)	15.72 (12.44–17.61)	13.07 (11.29–16.03)	15.16 (10.78–17.72)	15.12 (11.07–18.22)	n.a
Weight (kg)	64.5 (35–98.4)	52.5 (30–74)	61 (35.8–95)	51.8 (32–89.6)	$p = 0.0136$ (c-AEFI vs HC) $p = 0.0321$ (c-AEFI vs MIS-C)
BMI (kg/m^2)	22.68 (14.38–33.06)	20.26 (13.74–26.45)	21.98 (15.85–33.66)	18.49 (16.33–29.02)	n.a.
CRP (mg/dL)	0.83 (0–9.36)	16.44 (6.68–27.37)	0.08 (0.02–9.77)	0.05 (0.03–1.33)	$p < 0.001$ (MIS-C vs CoV-2+) $p < 0.001$ (MIS-C vs HC) $p < 0.001$ (c-AEFI vs MIS-C)
hs- TnT (pg/mL)	168 (3.6–2104)	76.8 (3–269)	3.8 (3–11.1)	n.a.	$p < 0.001$ (c-AEFI vs CoV-2+) $p = 0.0158$ (MIS-C vs CoV-2+)
NT-proBNP (pg/mL)	105.65 (18.2–1591)	2237.5 (36.1–34,250)	22.4 (5–311)	n.a.	$p < 0.001$ (MIS-C vs CoV-2+) $p = 0.0103$ (c-AEFI vs MIS-C)
Albumin (g/dL)	4.3 (4.2–4.6)	3.9 (2.6–4.9)	4.3 (3.8–5)	4.95 (4.5–5.2)	$p < 0.001$ (CoV-2+ vs HC) $p < 0.001$ (c-AEFI vs HC) $p = 0.0016$ (MIS-C vs HC)
Ferritin (ng/mL)	103.5 (74–196)	465 (14–23,345)	122.5 (35–919)	23 (4–190)	$p < 0.001$ (MIS-C vs HC)
PCT (ng/mL)	0.05 (0–0.15)	2.14 (0.03–18.66)	0.04 (0.02–0.54)	NA (Inf - -Inf)	$p = 0.0018$ (MIS-C vs CoV-2+) $p = 0.0032$ (c-AEFI vs MIS-C)

Table 1: All data are shown as median with minimum and maximum value. Body mass index (BMI); White Blood Cells (WBC); Large Unstained Cells (LUC); Hemoglobin (Hb); Erythrocyte Sedimentation Rate (ESR); C Reactive Protein (CRP); Creatine phosphokinase (CPK); Troponin T, High Sensitivity (hs-TNT); N-terminal prohormone of brain natriuretic peptide (NT-proBNP); Sodium (Na); Potassium (K); Aspartate Aminotransferase (AST); Alanine Aminotransferase (ALT); Gamma-glutamyltransferase (GGT); High-density lipoprotein (HDL); Low-density lipoprotein (LDL); Procalcitonin (PCT).
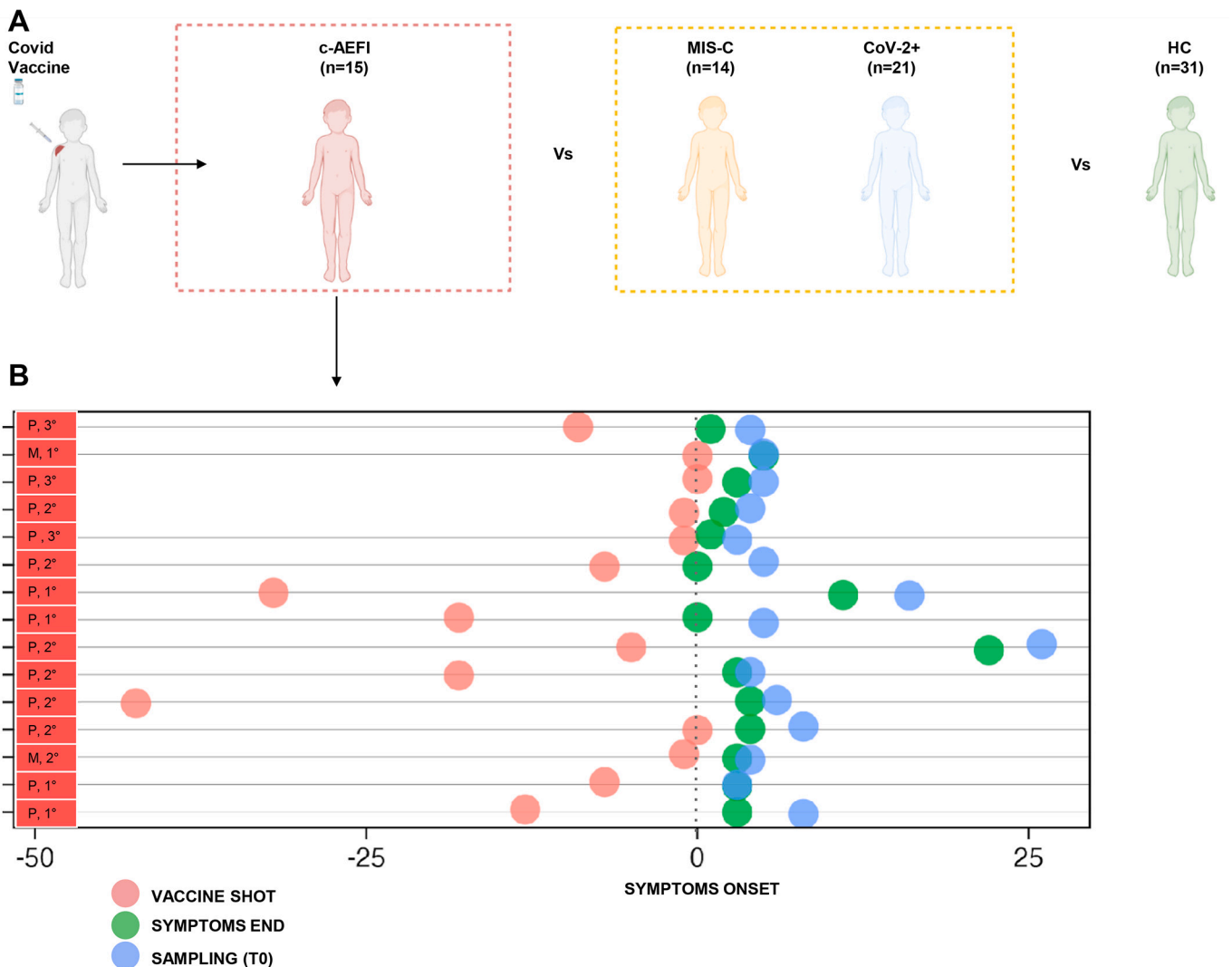
Fig. 1. Study cohorts and timeline.
A: Cohorts analyzed with sample size. c-AEFI: cardiac adverse event following immunization; MIS-C: Multisystem inflammatory syndrome in Children; CoV-2+: Children with Covid-19; HC: Healthy control; **B**: Timeline highlighting the time between the Vaccine shot and symptoms onset, the duration of symptoms and the time of sampling. Letters and numbers refer to the type of vaccine administered and the dose following which cardiac event was registered. P: Comirnaty Vaccine; M: Spikevax vaccine; 1°: first dose; 2° second dose; 3° third dose.

2.3. Hormone analyses by mass spectrometry

Steroid hormones have been measured using liquid chromatography coupled to tandem mass spectrometry (LC-MS/MS) method using the Xevo TQ-Smicro Mass Spectrometer of Waters. The preparation of the samples was carried out using the CE-IVD certified diagnostic kit of Chromsystems (Munich, Germany), while the processing of samples by using a Mass Spectrometer equipped with an ACQUITY UPLC I-Class liquid chromatograph that allows the realization of an ultra-high performance and low dispersion liquid chromatography (optimized to derive maximum benefits in terms of resolution and sensitivity) and a triple quadrupole that complies with Directive 98/79 / EC in all its parts.

We considered for each androgen level, except for 21-Deoxycortisol, the normal values reported on the datasheet of chromsystems (Chromosystems instruments & chemicals GmbH PR 72000 IT 08/2016 V5) according to age and gender.

2.4. Anti-heart muscle and anti-endothelial cell autoantibodies detection

An indirect immunofluorescence procedure with Heart muscle (Monkey) and human umbilical vein endothelial cells (HUVEC) as

substrates was performed. We used the TITERPLANE technique elaborated by EUROIMMUN.

Human umbilical vein endothelial cells cultures and primate heart muscles were incubated for 30 min with diluted 1:100 sera from patients on biochip platforms. After incubation, platforms were rinsed with a PBS-Tween wash buffer. During the second stage of incubation AECA or HMA antibodies (anti-endothelial cell antibodies or anti-heart muscle antibodies) bound to the substrate were identified by goat anti-human IgG antibodies marked with fluorescein (30 min in room temperature), and the rinsed again with PBS-Tween wash buffer.

Microscopic evaluation was performed by fluorescent microscope Nikon TS100.

2.5. HLA typing

The HLA typing was performed using next-generation sequencing (AllType NGS, One Lambda, Canoga Park, California) on the Ion Torrent Platform S5, (Thermo Fisher Scientific, Waltham, Massachusetts) while reads were analyzed by TypeStrem Visual software (Version 2.1), ranging from exons 1 to 8. In addition, the HLA typing was performed using another sequencing (NGSgo® MX11–3 kit, GENDX Yalelaan

Utrecht, Holland), method supported by the iSeq 100 platform (Illumina, San Diego, CA, USA), while the readings were analyzed by NGSengine software (version 2.26).

2.6. Statistical analysis

The clinical table presented data as median and range (min-max). The proteomics data were provided in NPX on a log2 scale where a high NPX represents high protein concentration.

For each continuous variable's distribution, normality was assessed using the Shapiro test, while variance homogeneity between distributions was evaluated using the Barlett test if all distributions were normally distributed; conversely was used the Fligner test.

Statistical comparisons of proteomics, androgens, and continuous clinical variables between more than two groups were performed using: the One-way ANOVA followed by Tukey-Kramer's post hoc test if the distributions were normally distributed and homogeneous, the Welch ANOVA followed by Games-Howell's post hoc test if the variances were unequal, but the distributions were normally distributed, and the Kruskal-Wallis's test followed by Dunn's post hoc test if the distributions weren't normally distributed. The post hoc tests were applied only on the variables with ad p-value adjusted (FDR) < 0.05.

Differences between two groups (HC vs. c-AEFI T1) were evaluated using the t-test if both the distributions were normally distributed and homogeneous, the Welch t-test if the variances were unequal, but the distributions were normally distributed, and the Mann-Whitney test if the distributions weren't normally distributed.

Correction for multiple comparisons was addressed by adjusting the p-values with the False Discovery Rate (FDR) method. Results were considered statistically significant for those with a p-value adj < 0.05. Categorical clinical data were conversely compared using Fisher's exact test [29]. To highlight the weight of the differentially produced proteins, we plotted a ranking calculated as -log10(Adjusted p-value)*log2(Fold Change). Rank is proportional both to significance and to the magnitude of the difference. We performed a Principal Component Analysis (PCA) on proteomics data to overview the patient's distribution in terms of plasma proteomics profile. Spearman's correlation was used to examine the association between variables.

Statistical analyses were performed using R (version 4.1.1).

To minimize the impact of age in this work we selected study participants who were between the ages of 10 to 19 years in each group. Furthermore, age distributions are approximately equally distributed and have no statistically significant differences between groups. Since, androgens levels are strongly influenced by gender, we measured androgens only in a subset of study participants in order to maintain a proportion of males and females similar to the c-AEFI group:

c-AEFI (2F/15), CoV-2+ (2F/9), HC (5F/22), MIS-C (2F/13).

2.7. Machine learning

To investigate the features exclusively different in the c-AEFI group against the subjects of all other groups and to correctly classify c-AEFI patients based on these features, we applied a Machine Learning (ML) approach. We merged proteomics, androgens, and continuous clinical data in a unique dataset of 163 features. Since proteomics data were in log2 scale, to uniform the dataset, we transformed in log2 scale also the other variables. Variables with missing data of $\geq 20\%$ were removed, so we reduced the number of features to 105. Using the two groups' differential pipeline described before, we applied the first step of features selection, which selected 24 variables. Data were scaled and centered, and the remaining missing values were imputed using the k-nearest neighbor (k−NN) method provided by the R caret package [30]. The final dataset of 81 patients (15 c-AEFI and 66 Others) was split into the training (60%) and testing (40%) datasets. Using the rfeControl function (caret package), we applied the Random Forest-Recursive Feature Elimination algorithm (RF-RFE) with 5-time repeated 10-fold cross-

validation on the training dataset to further reduce the number of variables to 20 that fed the model. Seventeen out of these 20 variables were further used by the model. Four ML algorithms were used, including Logistic Regression, Random Forest, eXtreme Gradient Boosting (XGBoost) and k-nearest neighbor (k-NN). In the training step of each algorithm, the optimal hyperparameters were selected by the random search method, and the 5-time repeated 10-fold cross-validation was used as a resampling method. Accuracy, sensitivity, and specificity computed on the testing dataset were used to evaluate the models. According to these parameters, the XGBoost model shows the best performance with an accuracy of 0.91, a specificity of 0.96, and a sensitivity of 0.67.

3. Results

3.1. Cohort characteristic

Age, gender, clinical, and main routine laboratory characteristics of the cohort are described in Table 1.

Out of the 15 patients affected by post vaccination myopericarditis (c-AEFI), 6 were classified as acute myocarditis, 3 as acute pericarditis and 6 as acute myo-pericarditis.

Thirteen out of 15 c-AEFI patients were male, 2 were female. The median age was 15.72 (12.44–17.61) years. The median onset of symptoms after vaccination was 7 days (range from 0 days to 41 days) while the median duration of the symptoms was 3 days (range from 1 to 22 days) (Fig. 1B).

Out of the 13 patients who received the Comirnaty vaccine, 4 showed symptoms after the first dose, 6 after the second and 3 after the third dose (Fig. 1B). Only 2 patients had been vaccinated with Spikevax, with reactions after the first and second dose respectively.

All patients but 3 were naïve to SARS-CoV-2 infections as demonstrated by the absence of SARS-CoV-2 anti-nucleocapsid (N) protein Abs. These 3 patients presented symptoms after the first dose of vaccine (two with Comirnaty and one with Spikevax respectively, Fig. 1B).

From a clinical perspective, 6 out of 15 patients presented a ST-segment elevation at ECG, 2 patients ST-segment depression and 1 patient T-wave inversion. The most frequent finding at echocardiogram was pericardial effusion, present on admission in 9 patients. In three patients, pericardial hyper-echogenicity was observed and only 1 patient showed global left ventricular (LV) systolic dysfunction, with ejection fraction (EF) of 45%.

In 5 patients out of 15, cardiac magnetic resonance Imaging (cMRI) was performed on admission and showed signs of myocarditis/myopericarditis in all. A 3–6 months follow-up cMRI was performed in 9 out of 15 patients, while 6 patients refused further investigations. Six out of the nine patients evaluated showed cardiac involvement defined according to the Lake Louise criteria [31].

An almost complete description of the cohort has been recently published [20]. Two additional patients were enrolled following the publication of the previous cohort. The cohort of patients with MIS-C consisted of 14 individuals, including 3 females and 11 males. The median age of patients in the MIS-C group was 13.07 years, ranging from 11.29 to 16.03 years. The median body mass index (BMI) for individuals in the MIS-C group was 20.26 kg/m^2, with a range of 13.74 to 26.45 kg/m^2. To better clarify the pathogenesis of different conditions with cardiac involvement we selected MIS-C patients with increased High Sensitivity Troponin (hs-TNT) value. Indeed, the median hs-TnT level among MIS-C patients was 76.8 pg/mL. The inflammation status was also confirmed by increased levels of CRP and ferritin (Table 1).

As described above, to avoid the potential confounding factor of age, we selected age and pubertal stage matched patients: 21 children with acute SARS-CoV-2 infection (CoV-2+), 14 children with MIS-C and 31 healthy children without any manifestation of acute or inflammatory disease enrolled in the pre-pandemic era (HC) were used for comparison. Cohort's clinical and routine laboratory characteristics at baseline are

reported in Table 1 and Supplementary Table S1.

3.2. Plasma proteomic profiles

Hyperimmunity has been involved in the pathogenesis of myocarditis after COVID-19 vaccination [32,33], but its role has not been yet clearly defined. We explored the inflammation status using the Inflammation panel of Olink® platform of patients developing myocarditis following mRNA COVID-19 vaccination, comparing them to other SARS-CoV2 associated conditions (14 patients with MIS-C and 21 patients CoV-2+) or HC (31).

After filtering out proteins with >20% measurements below the threshold of detection, principal component analysis (PCA) was able to distinguish MIS-C from myocarditis suggesting a distinct inflammatory profile between the two conditions (Fig. 2A).

Fig. 2B shows the intersections of proteins found differentially produced for the 5 comparisons evaluated. There were 12 proteins differentially expressed between c-AEFI and MIS-C, 18 proteins between c-AEFI and CoV-2+ and 18 proteins between c-AEFI and HC (Fig. 2C).

The main contributing features explaining the differences between c-AEFI and the other groups, included higher levels of CXCL5, STAMBP, SIRT2, AXIN1, GDNF and IL-10RB and lower levels of IL-10, CXCL10 and CXCL-11 (Fig. 2C). Circos plot in Fig. 2D highlights differentially expressed proteins (DEPs) found in c-AEFI vs MIS-C and 4 proteins with important biological functions resulting significant in comparison to HC: CXCL11 ($p = 0.19$, fold-change -1.19), STAMBP ($p = 0.09$, fold-change 1.7), AXIN1 ($p = 0.2$ fold-change 1.6), SIRT2 ($p = 0.37$, fold-change 1).

c-AEFI patients expressed the highest STAMBP (deubiquitinase STAM binding protein) level compared to all the other groups (although not statistically significant when compared to MIS-C).

We also found in MIS-C a significantly lower level of CXCL5 compared to c-AEFI. On the other hand, SIRT2 (Sirtuins 2), a NAD + -dependent deacetylase involved in the inhibition of pathological cardiac hypertrophy and ischaemia-reperfusion injury [34], was found higher in c-AEFI, MIS-C and Cov-2+ compared to HC with the highest level in the c-AEFI group (supplementary fig. S1). Moreover, BMI in c-AEFI cohorts was negatively correlated with SIRT2, confirming the major predisposition to oxidative stress in overweight children (data not
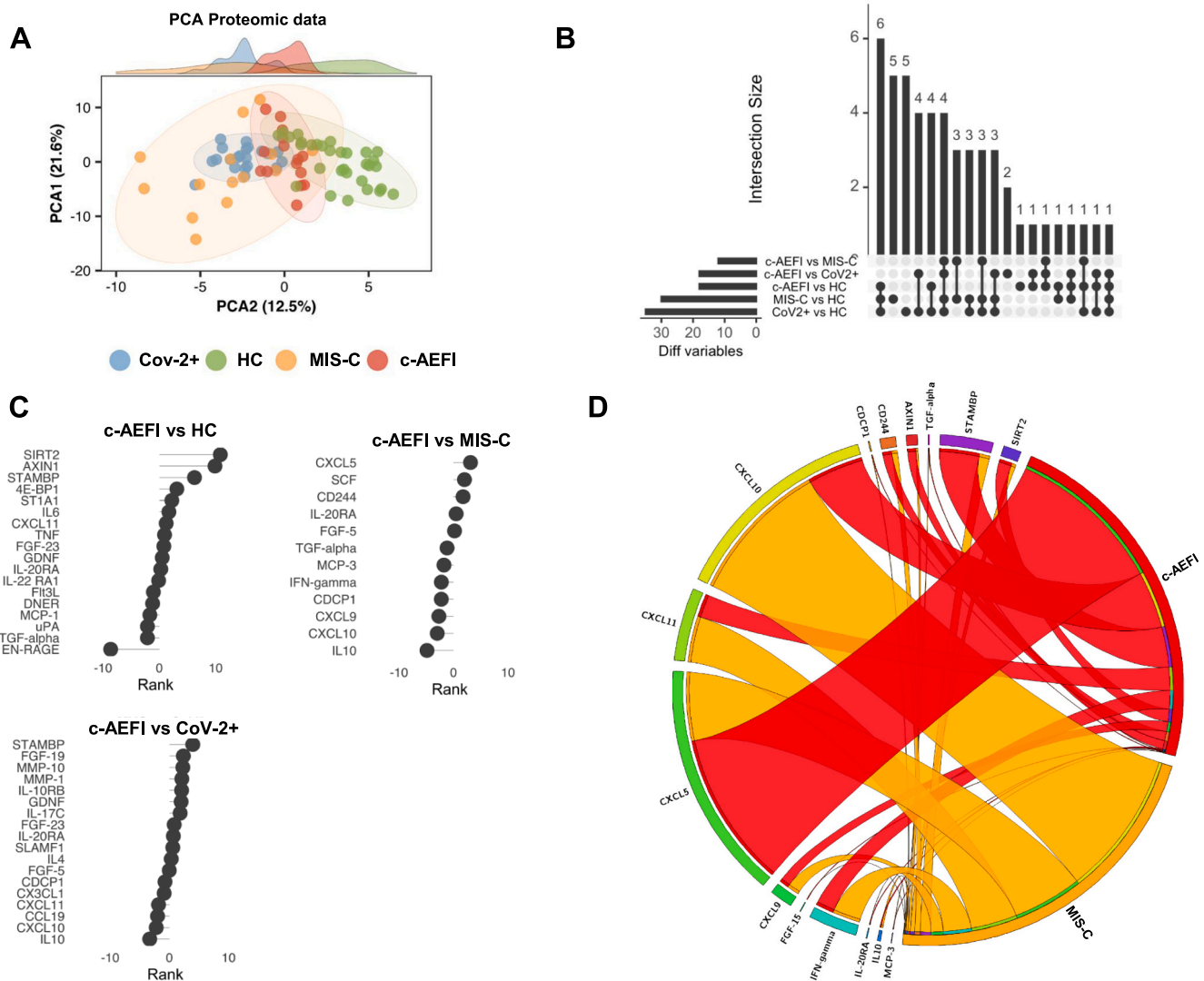

Fig. 2. Proteomic Analysis.
A: PCA analysis of proteomic data in the groups analyzed; **B**: The intersection graph highlights the proteins found differentially produced that are common across different comparisons; **C**: Proteins differentially expressed (DEPs) between c-AEFI and other groups. Rank value is calculated as -log10 of *p*-value adjusted x log2 fold change; **D**: Circos plot representing both DEPs between MIS-C and c-AEFI and protein with important biological function resulting significant in comparison to HC; values are plotted as 2^NPX.

shown). IL-6 has been shown to play a role in patients with complicated Covid-19 compared with patients with uncomplicated disease [35]. In line with these data, our analysis shows a similar IL-6 over-expression in both c-AEFI and MIS-C. However, other systemic pro-inflammatory cytokines [36], such as CXCL9, CXCL10 and IFN-gamma were found higher in MIS-C and able to distinguish these two conditions (Fig. 2C and supplementary fig. S1). Indeed, both were found higher in MIS-C.

We also identified additional plasma proteins distinguishing HC from the other groups. One of these was the pro-apoptotic protein AXIN1 [37], which was most elevated in c-AEFI (Fig. 2C and Supplementary fig. S1). We further found a reduced level of IL-10, an anti-inflammatory cytokine, which resulted significantly lower in c-AEFI compared to

MIS-C and CoV-2+. Figs. 2C and supplementary fig. S2 show protein comparison among the groups. In order to track down the dynamics of such cytokine perturbation we also performed an additional proteomic analysis within the c-AEFI cohort at a longer follow-up ranging from 1 to 6 months. In Fig. 3 we show proteins decreasing during the follow-up. Most proteins depicted are key proteins in the inflammatory response while we do not observe any decrease in the above mentioned proteins involved in the cardiomyocyte damage.

3.3. Androgens levels in myocarditis patients

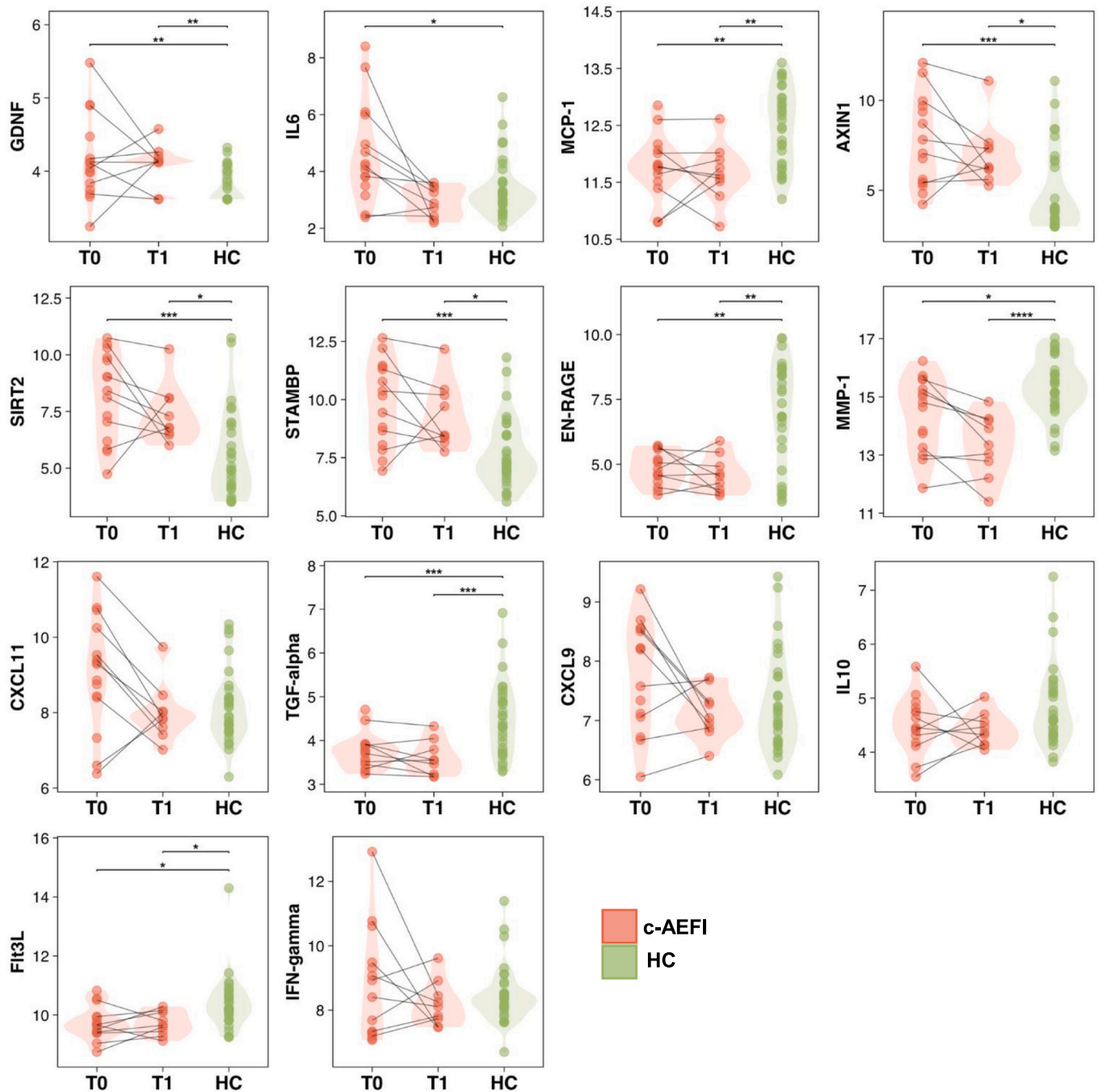Based on the findings that males had a higher incidence of

Fig. 3. Proteomic Analysis over time.
Proteomics longitudinal analyses of c-AEFI at two different timepoints compared to HC. Violin plots represent the three group's distribution. Each line between c-AEFI timepoints represents the protein level trajectory for an individual patient.

myocarditis following SARS-CoV-2 infection and vaccination, it was proposed that androgens could have a potential role post COVID19 vaccination cardiac events [16,32]. Moreover, the role of androgens in the immune system has been largely investigated [38]. In line with this, we analyzed the level of androgens in our cohort and, considering the variability of androgen levels, we performed an additional selection of the control groups according to age and gender in order to increase the reliability of the results.

We compared androgen levels in 15 c-AEFI, 13 patients with MIS-C, 9 CoV-2+ and 22 HC.

We found statistically significant different levels of testosterone, DHEAS, DHEA, androstenedione and cortisone (Table 2 and Fig. 4A) between the groups. MIS-C patients showed the lowest values of these hormones in comparison to all other groups. Higher levels of 21-Deoxycortisol were expressed in c-AEFI and CoV-2+ than HC. c-AEFI patients showed the highest level of DHEAS which resulted statistically significant when compared to both MIS-C and HC. Lower levels of Corticosterone were found in c-AEFI and MIS-C than HC.

We also analyzed the sex hormone binding protein (SHBG) to exclude its known effect on androgens bioavailability. We did not find any correlation between SHBG and androgens level (data not shown), confirming the reliability of our results. Interestingly, Androstenedione in c-AEFI cohort was positively correlated with BMI ($p = 0.004$, rho = 0.7, data not shown). Given these results, we wondered if the observed distribution could represent a consequence of hormone perturbation caused by the inflammatory status itself or could be present before the onset of myocarditis symptoms. We therefore analyzed androgens levels during a follow-up ranging between 1 and 6 months after symptoms onset. Our analysis showed that c-AEFI expressed higher DHEAS, DHEA and cortisone levels compared to HC, which persist after a longer follow-up (Fig. 4B).

3.4. Autoantibodies analysis

Considering the possible role of autoimmunity in myocarditis pathogenesis we eventually detected anti-heart muscle and anti-endothelial cell antibodies.

Five out of 15 patients in the c-AEFI cohort showed presence of autoantibodies. Two patients resulted positive for anti-heart muscle antibodies and two for anti-endothelial antibodies. Finally, one patient reported double positivity for both auto-antibodies. In the CoV-2+ cohort, 3 patients resulted positive for anti-endothelial antibodies, 2 patients for anti-heart muscle and two patients resulted positive for both autoantibodies. In the MIS-C cohort only two patients turned positive for anti-endothelial autoantibodies. Finally, the detection of autoantibodies in the HC cohorts was possible for anti-endothelial autoantibodies only due to plasma availability and 5 individuals resulted positive (Fig. 5A).

3.5. HLA typing

Given previous studies suggesting a genetic susceptibility to MIS-C [39,40], we performed HLA-typing in children developing myocarditis following vaccination. Our results showed an HLA distribution similar to the general population and did not highlight any specific HLA association in the cohort analyzed in contrast to those reported in MIS-C patients in larger studies.

Machine learning (ML) Analysis to explore distinctive features of post-vaccination cardiac events.

We aimed to define distinctive features of post-vaccine cardiac events as compared to MIS-C, healthy control and COVID19 pediatric patients (total of 81 patients) exploring a ML model. To do so we fed the model with proteomics, androgens, and continuous clinical data in a unique dataset of 163 features. Differential analysis between the group
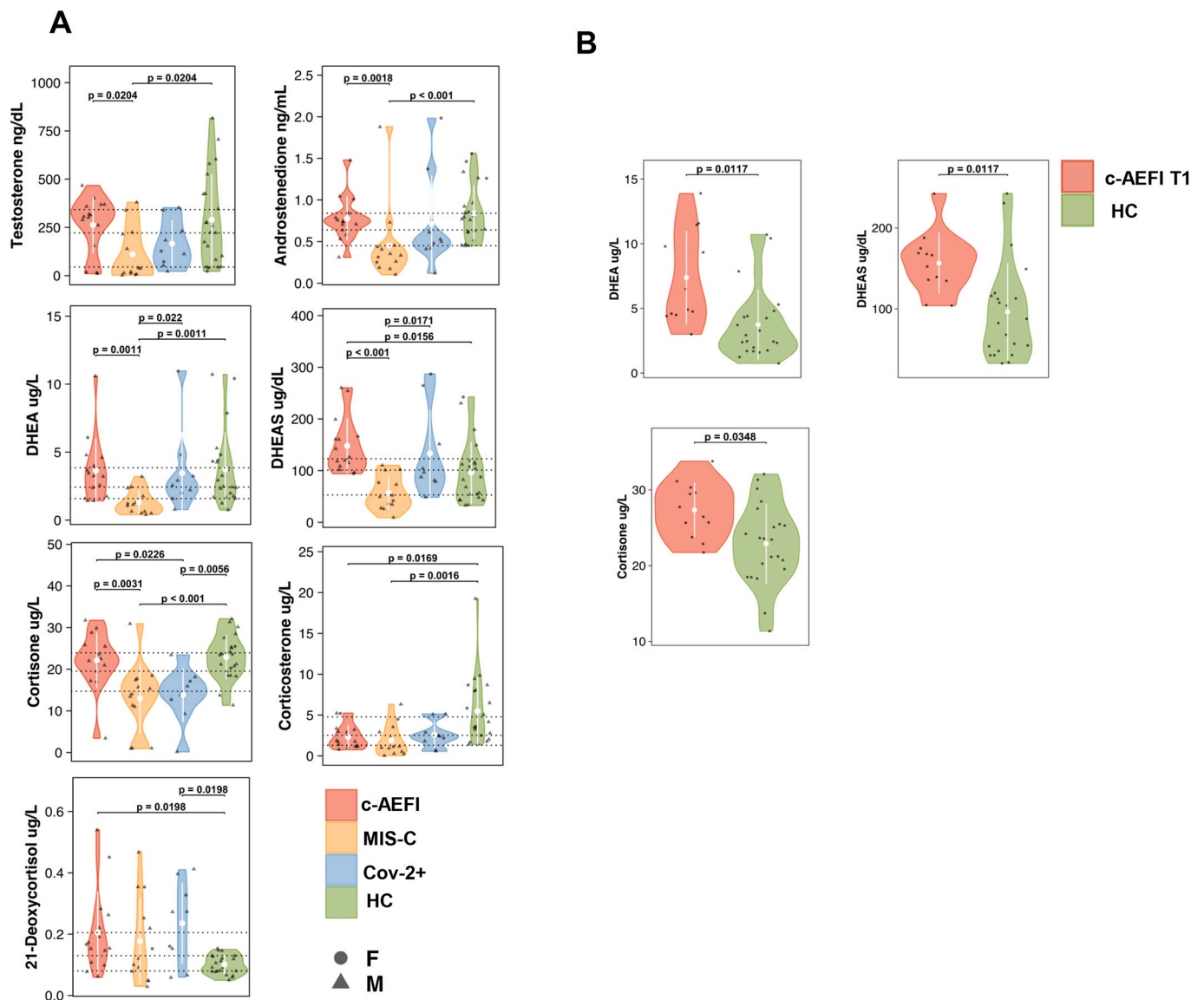
Table 2
Hormones' profile of the cohort.

	c-AEFI	MIS-C	CoV2+	HC	p-value
DHEA	3.25	1.14	2.55	2.7	p = 0.0011 (c-AEFI vs MIS-C)
(ug/L)	(1.42–10.59)	(0.4–3.2)	(0.78–10.96)	(0.75–10.71)	p = 0.0011 (MIS-C vs HC)
					p = 0.022 (MIS-C vs CoV-2+)
DHEAS	126.05	49.39	96.69	85.05	p < 0.001 (c-AEFI vs MIS-C)
(ug/dL)	(94.16–260.24)	(9.12–110.29)	(48.55–287.03)	(32.75–242.4)	p = 0.0156 (c-AEFI- vs HC)
					p = 0.0171 (MIS-C vs CoV-2+)
Androstenedione (ng/mL)	0.74	0.33	0.5	0.78	p < 0.001 (MIS-C vs HC)
	(0.31–1.48)	(0.1–1.88)	(0.12–1.98)	(0.45–1.56)	p = 0.0018 (c-AEFI vs MIS-C)
Testosterone	305	37	127	240.2	p = 0.0204 (c-AEFI vs MIS-C)
(ng/dL)	(10–467)	(2–380)	(22–352)	(22.2–815.8)	p = 0.0204 (MIS-C vs HC)
DHT	0.17	0.07	0.1	0.12	n.a
(ug/L) nr	(0.05–0.35)	(0.02–0.21)	(0.05–0.31)	(0.01–0.55)	
Progesterone	0.22	0.18	0.26	0.41	p = 0.0074 (MIS-C vs HC)
(ng/mL)	(0.12–0.62)	(0.09–0.31)	(0.12–1.95)	(0.09–6.55)	
11-Deoxycorticosterone (ug/L)	0.04	0.03	0.03	0.06	p = 0.0152 (MIS-C vs HC)
	(0.02–0.06)	(0.01–0.07)	(0.02–0.08)	(0.02–0.31)	p = 0.0492 (c-AEFI vs HC),
					p = 0.0492 (CoV-2+ vs HC)
Corticosterone	1.76	1.14	2.41	3.9	p = 0.0016 (MIS-C vs HC)
(ug/L)	(0.77–5.23)	(0.03–6.32)	(0.58–5.13)	(1.41–19.25)	p = 0.0169 (c-AEFI vs HC)
17-OH-Progesterone (ng/mL)	0.97	0.37	0.47 (0.24–1.39)	0.78	n.a
	(0.18–2.21)	(0.1–1.57)		(0.23–2.16)	
21-Deoxycortisol	0.17	0.12	0.27	0.1	p = 0.0198 (c-AEFI vs HC)
(ug/L)	(0.06–0.54)	(0.03–0.47)	(0.06–0.41)	(0.05–0.15)	p = 0.0198 (CoV-2+ vs HC)
11-Deoxycortisol	0.64	0.44	0.63	0.4	n.a
(ug/L)	(0.07–1.71)	(0.02–1.8)	(0.03–1.36)	(0.12–1.58)	
Cortisol	112.77	112.06	132.68	115.84	n.a
(ug/L)	(67.54–358.75)	(5.03–217.69)	(7.81–319.44)	(54.42–280.23)	
Cortisone	22.09	14.02	14.09	23.5	p < 0.001 (MIS-C vs HC)
(ug/L)	(3.43–31.75)	(0.96–30.91)	(0.18–23.44)	(11.36–32.08)	p = 0.0031 (c-AEFI vs MIS-C)
					p = 0.0056 (CoV-2+ vs HC)
					p = 0.0226 (c-AEFI vs CoV-2+)
SHBG (nM/L)	12.4	n.a.	n.a.	n.a.	n.a
	(6.86–31.1)				

Table 2: All data are shown as median with minimum and maximum value. Dehydroepiandrosterone (DHEA); dehydroepiandrosterone sulfate (DHEAS); dihydrotestosterone (DHT); Sex Hormone Binding Globulin (SHBG).

Fig. 4. Androgenic Profiles in Myocarditis, MIS-C, SARS-CoV-2+ and Healthy Control.
A: Violin plots represent androgens level in the cohort analyzed. Black dashed lines represent the first quartile, the median, and the third quartile of the compressive distribution, respectively from below. For each distribution, in white is visualized the error bar (mean ± SD); **B**: Cortisone, DHEA and DHEAS levels analyzed in the c-AEFI patients during follow-up period and Healthy controls. In white are visualized the error bars (mean ± SD).

and Random Forest Recursive Feature Elimination were able to narrow down the most informative features to 17 variables (Fig. 5B). These features were afterwards used in a training set made of 60% of the group and later tested on the remaining 40% (pipeline shown in Fig. 5B). The XGBoost model showed the best performance compared to the other model tested, with an accuracy of 0.91, a specificity of 0.96, and a sensitivity of 0.67. Whereas this approach was limited by the small sample size and the consequent risk of overfitting, it suggested that this approach, if repeated on a larger dataset may help distinguish this condition from others and possibly anticipate any type of intervention. The features suggested by the model, ranked by importance in Fig. 4B, are few proteins already found in the differential analysis, such as SIRT2, IL10RB, STAMBP and IL-17C found higher in c-AEFI, and IL10 and TGF alpha found significantly lower in the c-AEFI compared to other groups. Despite the control groups being all matched for age, also the model suggested that weight and BMI were among the most informative features to define c-AEFI as compared to MIS-C, CoV-2+ and Healthy controls. This approach, possibly limited by the age and gender matched control groups, will need to be further tested on an unsupervised cohort

to confirm the performance of the model.

4. Discussion

The risk of acute myocarditis associated with COVID-19 mRNA vaccination is attracting great attention and is a matter of debate, especially in the pediatric population where the benefit-risk must be carefully evaluated [41,42]. The pathogenesis of COVID-19 mRNA-vaccination-related myocarditis still remains poorly understood and potentially recognizes several mechanisms. Among these, mRNA immune reactivity, cross-reacting antibodies to SARS-CoV-2 spike glycoproteins with myocardial contractile proteins and hormonal differences have been suggested as significant in the subsequent development of c-AEFI [7,32]. Clinical and demographic characteristics of our cohort are in line with previously published case series [7,10,15,32,43], including the type of vaccine administered, the triggering dose and the male/female ratio. Interestingly, all patients developed symptoms following the 2nd or 3rd dose except those who already experienced SARS-CoV-2 infection, who developed symptoms after the first dose. This
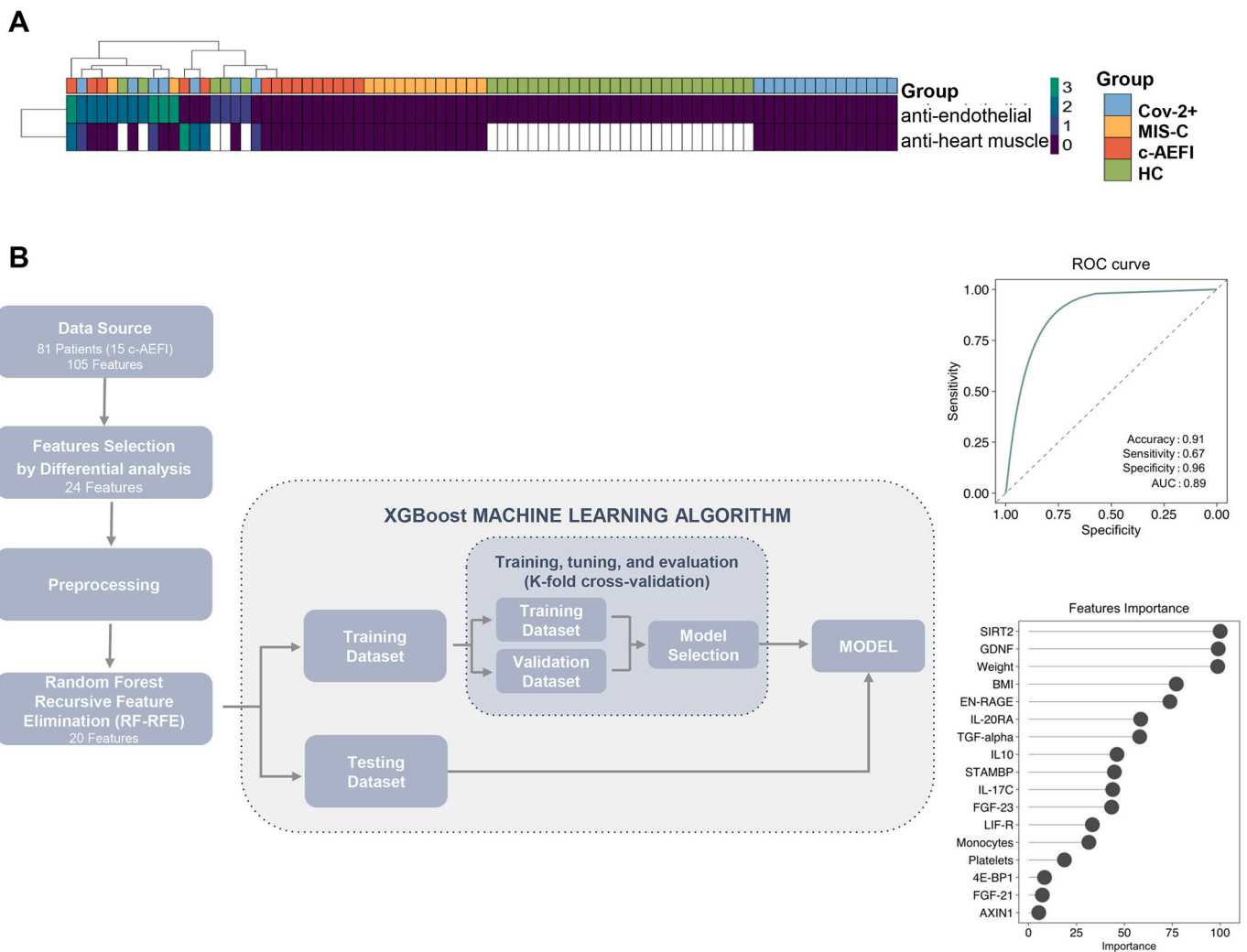
Fig. 5. Autoantibodies and Machine Learning model.

A: Hierarchical clustering of autoantibody activity against heart muscle and endothelial tissues. Color scale indicates if negative = 0, low positivity = 1, intermediate positivity = 2, positivity = 3. White squares indicate unavailable data; **B**: Machine Learning model.

Cartoon shows the pipeline developed to build the predictive model aiming at defining features of myopericarditis. Data source was produced merging proteomics, androgens, and continuous clinical data in a unique dataset of 163 features. Differential analysis between the groups initially selected 24 variables, further narrowed to 20 applying the Random Forest-Recursive Feature Elimination algorithm (RF-RFE). Seventeen out of these 20 variables were further used to feed the model on the training set of the entire cohort (60% of the entire cohort; $n = 81$; c-AEFI = 15; Other groups $n = 66$). Four ML algorithms were used, including Logistic Regression, Random Forest, eXtreme Gradient Boosting (XGBoost) and k-nearest neighbor (k-NN). Accuracy, sensitivity, and specificity computed on the testing dataset of patients (40% of the entire cohort) were used to evaluate the models and are shown in the ROC curve in the upper right panel. Lower right panel shows the ranking for importance of features used in the model.

observation suggests that previous exposure to spike protein may play a role in the pathogenesis of this condition.

We explored the inflammatory features of pediatric patients developing myocarditis following mRNA COVID-19 vaccination, by combining clinical and routine laboratory data along with high-dimensional proteomic analysis. c-AEFI patients were compared to children with MIS-c and cardiac involvement, SARS-CoV-2 infected children and healthy controls. Overall, we found a heart restricted inflammation in children experiencing c-AEFI in comparison to the other groups. The expression of proteins involved in stress-induced cardiomyocyte apoptosis, cardiac oxidative stress and myocardial injury in both acute ischaemic and non-ischaemic damage suggest a restricted heart inflammation. Indeed, SIRT2 plays a protective role on endothelial damage according to the level of Reactive oxygen species (ROS). SIRT2, belonging to the family of sirtuins proteins, is a NAD + -dependent deacetylases and is involved in the inhibition of pathological cardiac hypertrophy and ischaemia-reperfusion injury with different effects

according to the level of oxidative stress [34]. On the other hand, the higher level of SIRT2 found in myocarditis could be related to the direct cardiomyocyte damage as also found by others during acute myocardial infarction [34,44,45]. The myocardial inflammation could explain the increased level of SIRT2. ROS level can modulate cardiac damage with multiple mechanisms. Some evidence suggests a protective role of monocyte chemoattractant protein-1 (MCP-1) in the pathophysiology of ischaemic heart disease through a ROS-dependent pathway [46,47]. Interestingly, several factors proved to be protective for the cardiac damage in murine models such as MCP-1, GDNF, uPA, Flt3L [48–51] resulted differentially expressed in c-AEFI in comparison to HC (Fig. 2) opening the question if these levels may be indicative of a predisposition to develop myocarditis.

A more heart-restricted inflammation in patients with c-AEFI was also suggested by a higher level of STAMBP. Indeed, STAMBP through the regulation of NLRP3 inflammasome [52,53] acts on myocardial injury provided by both ischaemic and non-ischaemic damage [54].

Thus, a high STAMBP level may represent an attempt to downregulate inflammation through the NLRP3 pathway. Conversely, a key anti-inflammatory factor such as IL-10 [55–57], which is increased in MIS-C patients in order to control the ongoing systemic inflammation was shown to not increase in c-AEFI. Indeed MIS-C patients expressed the highest abundances of key-proteins in the systemic inflammation. In line with previous data we found the highest level of CCL19, CXCL10, and CDCP1 [58], IFN-gamma and IL-6. In contrast, the MIS-C cohort expressed the lowest level of CXCL5, a potent neutrophil chemoattractant and activator [59] whose level has been found low in some inflammatory conditions [60].

Noteworthy, the proteins directly involved in the cardiomyocyte damage (AXIN-1, SIRT2, STAMBP) remained high even at the follow-up. The evidence of a reduction in the systemic inflammatory proteins over time (i.e. IL-6, IFN-gamma, CXCL9, CXCL11) in contrast to the molecules involved in cardiomyocyte damage which remain stable, suggest their potential role in the findings observed in the c-MRI of these patients over their follow-up. Collectively, these findings indicate a systemic inflammation in patients with MIS-C, as opposed to myocarditis where the inflammation is localized to the heart. According to this, CRP values were significantly higher in MIS-C compared to c-AEFI. Whereas, albeit not significant, a higher hs-TnT value was found in c-AEFI compared to MIS-C (Table 1). These data highlight the immune-mediated response occurring in myocarditis following vaccination where the immune system reacts to the viral protein fragments introduced by the vaccine, leading to inflammation in the heart muscle. In line with this hypothesis, Yonker L et al. recently reported that individuals who developed c-AEFI uniquely exhibit elevated levels of free spike protein in circulation, which appear to correlate with cardiac troponin T levels and innate immune activation with cytokine release [61]. Given the gender distribution of c-AEFI, largely reported also in other vaccines studies [62], and androgens ability to modulate inflammatory responses through several mechanisms [63], we analyzed their level across the cohorts in the acute phase.

An increased level of DHEAS, which persists in long term follow-up in patients with myocarditis in comparison to both MIS-C and HC was found. Some studies have shown a reduction in DHEAS levels in heart failure [64] and suggest that DHEA(S) may play an important physiological role in the prevention of cardiovascular disease [65]. Given the role of DHEAS in the immune system, specifically in the modulation of TH2 responses and IFN-gamma production and the promotion of IL-2 production [66,67] along with its role in cardiovascular diseases, a potential role in the pathogenesis of c-AEFI cannot be excluded. Indeed, despite the extensive literature on the vascular and metabolic effects of dehydroepiandrosterone, the relationship between DHEA/S levels and cardiovascular events remains uncertain and conflicting.

Interestingly, MIS-C subjects showed a partial defect on the steroidogenesis pathway involving mineralocorticoid production. In particular lower progesterone, testosterone, 11-deoxycorticosterone and corticosterone levels were observed compared to HC. Some evidence from the literature suggests a role of testosterone in the modulation of anti-inflammatory cells and Th1-type immune response [68–71]. Testosterone has been involved in several mechanisms potentially leading to fibrosis in the setting of myocarditis including inflammation [64,65,72]. These findings are consistent with hyponatremia and hypotension occurring in patients during the acute phase of MIS-C.

Autoantibody mediated heart inflammation was also evaluated. The absence of a clear pattern of cardiac targeted autoantibodies in c-AEFI cases in comparison to the other groups doesn't suggest an autoantibody mediated mechanism behind this condition. Our data are in line with recent available literature evidence [73,74]. These findings indicate that other factors or mechanisms may contribute to the development of myocarditis following vaccination. Among these, it has been recently reported that genetic host factors could play a role in the hyper-inflammation observed in some COVID-19 cases. Indeed Lee et al. [75] reported that variants in genes encoding the viral RNA sensing pathway

lead to exuberant inflammatory responses in myeloid cells in some individuals with MIS-C. Currently, it is still unexplored if such genes can also be involved in the pathogenesis of c-AEFI. Moreover, our HLA-typing analysis in children with cardiac events following immunization did not reveal any of the specific HLA association reported in larger studies on MIS-C patients [40], hence supporting the hypothesis of two distinct pathogenic conditions.

We further explored the multisystem approach in a machine learning model. Such a model was able to distinguish c-AEFI compared to other COVID-19 related conditions, including MIS-C suggesting that proteomic analysis, coupled with hormone profile and continuous clinical data may be used in the future to provide a predictive score of post-vaccination cardiac events. However, this observation, now limited by the small sample size will need to be further validated on larger cohorts.

Although the absolute number of patients with myocarditis enrolled is low, it must be taken into account the low frequency of myocarditis following vaccination and the fact that this is a monocentric study.

Overall, the present work showed a distinct inflammatory and androgenic profile in patients developing c-AEFI following mRNA vaccination which persists months after the acute event, whereas excluding a pathogenic role of autoantibodies. Larger international collaborative studies are needed in order to un-reveal the biological mechanisms and of immunopathology of c-AEFI following COVID vaccination.

Author contributions

Conceptualization, D.A., P·P.; Methodology, D.A., G.R.P. and P.P; Software, G.R.P.; Formal analysis, G.R.P. and D.A.; Investigation, D.A., C.P., E.M., E.C.M., A.D., M.A., C.R., N.C. and A.D.; Resources, C.P., E.M., A.D., A.V.; Data curation, G.R.P.; Writing – original draft, D.A., G.R.P., N.C., C.R. and E.C.M.; Writing – review & editing, D.A., G.R.P., N.C., C.R., E.C.M, M.A.P, M.C, A.F., A.D., S.C., M.A, O.P. and P.P.; Visualization, D.A., G.R.P., N.C., C.R., and E.C.M.; Funding acquisition, D.A., P.P., N.C.; Project administration, P.R. and P.P.; Investigation, D.A., C.R. G.R.P. N.C.; Supervision, P.R. and P.P.

Declaration of Competing Interest

The authors declare no competing interests.

Data availability

Data will be made available on request.

Acknowledgments

Appendix A. Supplementary data

Supplementary data to this article can be found online at https://doi.org/10.1016/j.clim.2023.109751.

References

[1] J. Abbasi, Medical News & Perspectives COVID-19 and mRNA Vaccines-First Large Test for a New Approach, 2020.

[2] T. Fiolet, Y. Kherabi, C.J. MacDonald, J. Ghosn, N. Peiffer-Smadja, Comparing COVID-19 vaccines for their characteristics, efficacy and effectiveness against SARS-CoV-2 and variants of concern: a narrative review, Clin. Microbiol. Infect. 28 (2022) 202–221.

[3] S. Sagar, P.P. Liu, L.T. Cooper, Myocarditis, Lancet 379 (2012) 738–747.

[4] A. Arola, E. Pikkarainen, J.O. Sipilä, J. Pykäri, P. Rautava, V. Kytö, Occurrence and features of childhood myocarditis: a nationwide study in Finland, J. Am. Heart Assoc. (2017) 6.

[5] J.R. Su, M.M. McNeil, K.J. Welsh, et al., Myopericarditis after vaccination, vaccine adverse event reporting system (VAERS), 1990–2018, Vaccine 39 (2021) 839–845.

[6] Centers for Disease Control and Prevention (CDC), Advisory Committee on Immunization Practices (ACIP), Coronavirus Disease 2019 (COVID-19) Vaccines, Accessed July 6, 2021, https://www.cdc.gov/vaccines/acip/meetings/slides-202 1-06.html.

[7] B. Bozkurt, I. Kamat, P.J. Hotez, Myocarditis with COVID-19 mRNA vaccines, Circulation 144 (2021) 471–484.

[8] Centers for Disease Control and Prevention (CDC). https://wonder.cdc.gov/contro ller/datarequest/D8.

[9] D. Gubernot, A. Jazwa, M. Niu, et al., U.S. population-based background incidence rates of medical conditions for use in safety assessment of COVID-19 vaccines, Vaccine 39 (2021) 3666–3677.

[10] D. Mevorach, E. Anis, N. Cedar, et al., Myocarditis after BNT162b2 mRNA vaccine against Covid-19 in Israel, N. Engl. J. Med. 385 (2021) 2140–2149.

[11] G. Witberg, N. Barda, S. Hoss, et al., Myocarditis after Covid-19 vaccination in a large health care organization, N. Engl. J. Med. 385 (2021) 2132–2139.

[12] J. Montgomery, M. Ryan, R. Engler, et al., Myocarditis following immunization with mRNA COVID-19 vaccines in members of the US military, JAMA Cardiol. 6 (2021) 1202–1206.

[13] M. Wang, W. Wen, M. Zhou, C. Wang, Z.-H. Feng, Meta-analysis of risk of myocarditis after messenger RNA COVID-19 vaccine, Am. J. Cardiol. 167 (2022) 155–157.

[14] M.E. Oster, D.K. Shay, J.R. Su, et al., Myocarditis cases reported after mRNA-based COVID-19 vaccination in the US from December 2020 to August 2021, JAMA 327 (2022) 331.

[15] H.-L. Wong, M. Hu, C.K. Zhou, et al., Risk of myocarditis and pericarditis after the COVID-19 mRNA vaccination in the USA: a cohort study in claims databases, Lancet 399 (2022) 2191–2199.

[16] S. Le Vu, M. Bertrand, M.-J. Jabagi, et al., Age and sex-specific risks of myocarditis and pericarditis following Covid-19 messenger RNA vaccines, Nat. Commun. 13 (2022) 3633.

[17] L. Chouchana, A. Blet, M. Al-Khalaf, et al., Features of inflammatory heart reactions following mRNA COVID-19 vaccination at a global level, Clin. Pharmacol. Ther. 111 (2022) 605–613.

[18] L. Hoste, R. Van Paemel, F. Haerynck, Multisystem inflammatory syndrome in children related to COVID-19: a systematic review, Eur. J. Pediatr. 180 (2021) 2019–2034.

[19] L.R. Feldstein, E.B. Rose, S.M. Horwitz, et al., Multisystem inflammatory syndrome in U.S. children and adolescents, N. Engl. J. Med. 383 (2020) 334–346.

[20] E.C. Manno, D. Amodio, N. Cotugno, et al., Higher troponin levels on admission are associated with persistent cardiac magnetic resonance lesions in children developing myocarditis after mRNA-based COVID-19 vaccination, Pediatr. Infect. Dis. J. 42 (2023) 166–171.

[21] Centers for Disease Control and Prevention (CDC), Clinical Considerations: Myocarditis and Pericarditis after Receipt of mRNA COVID-19 Vaccines among Adolescents and Young Adults, Available at, https://www.cdc.gov/vaccines/covid -19/clinical-considerations/myocarditis.html. Accessed September 2, 2022.

[22] S. Jhamnani, A. Fuisz, J. Lindsay, The spectrum of electrocardiographic manifestations of acute myocarditis: an expanded understanding, J. Electrocardiol. 47 (2014) 941–947.

[23] E. Ammirati, M. Frigerio, E.D. Adler, et al., Management of Acute Myocarditis and Chronic Inflammatory Cardiomyopathy: an expert consensus document, Circ. Heart Fail. 13 (2020), e007405.

[24] P. Garg, P. Morris, A.L. Fazlanie, et al., Cardiac biomarkers of acute coronary syndrome: from history to high-sensitivity cardiac troponin, Intern. Emerg. Med. 12 (2017) 147–155.

[25] C.R. Consiglio, N. Cotugno, F. Sardh, et al., The immunology of multisystem inflammatory syndrome in children with COVID-19, Cell 183 (2020) 968–981.e7.

[26] N. Cotugno, A. Ruggiero, G.R. Pascucci, et al., Virological and immunological features of SARS-COV-2 infected children with distinct symptomatology, Pediatr. Allergy Immunol. 32 (2021) 1833–1842.

[27] D. Amodio, N. Cotugno, P. Palma, COVID-19 in children: from afterthought to unknown, Cell Rep Med 3 (2022), 100558.

[28] M. Lundberg, A. Eriksson, B. Tran, E. Assarsson, S. Fredriksson, Homogeneous antibody-based proximity extension assays provide sensitive and specific detection of low-abundant proteins in human blood, Nucleic Acids Res. 39 (15) (2011) e102, https://doi.org/10.1093/nar/gkr424. Epub 2011 Jun 6. PMID: 21646338; PMCID: PMC3159481.

[29] S.W. Lee, Methods for testing statistical differences between groups in medical research: statistical standard and guideline of life cycle committee, Life Cycle (2022) 2.

[30] M. Kuhn, Building predictive models in R using the **caret** package, J. Stat. Softw. 28 (2008).

[31] V.M. Ferreira, J. Schulz-Menger, G. Holmvang, et al., Cardiovascular magnetic resonance in nonischemic myocardial inflammation: expert recommendations, J. Am. Coll. Cardiol. 72 (2018) 3158–3176.

[32] S. Heymans, L.T. Cooper, Myocarditis after COVID-19 mRNA vaccination: clinical observations and potential mechanisms, Nat. Rev. Cardiol. 19 (2022) 75–77.

[33] A. Vojdani, D. Kharrazian, Potential antigenic cross-reactivity between SARS-CoV-2 and human tissue with a possible link to an increase in autoimmune diseases, Clin. Immunol. 217 (2020), 108480.

[34] M. Zheng, X. Du, L. Zhao, H. Sun, M. Chen, X. Yang, Elevated plasma Sirtuin2 level predicts heart failure after acute myocardial infarction, J Thorac Dis 13 (2021) 50–59.

[35] E.A. Coomes, H. Haghbayan, Interleukin-6 in Covid-19: a systematic review and meta-analysis, Rev. Med. Virol. 30 (2020) 1–9.

[36] D.R. Julian, M.A. Kazakoff, A. Patel, J. Jaynes, M.S. Willis, C.C. Yates, Chemokine-based therapeutics for the treatment of inflammatory and fibrotic convergent pathways in COVID-19, Curr Pathobiol Rep 9 (2021) 93–105.

[37] X. Ye, J. Lin, Z. Lin, et al., Axin1 up-regulated 1 accelerates stress-induced cardiomyocytes apoptosis through activating Wnt/β-catenin signaling, Exp. Cell Res. 359 (2017) 441–448.

[38] S.P. Prall, M.P. Muehlenbein, DHEA modulates immune function: a review of evidence, Vitam. Horm. 108 (2018) 125–144.

[39] R.A. Porritt, L. Paschold, M.N. Rivas, et al., HLA class I-associated expansion of TRBV11-2 T cells in multisystem inflammatory syndrome in children, J. Clin. Invest. 131 (2021).

[40] K. Sacco, R. Castagnoli, S. Vakkilainen, et al., Immunopathological signatures in multisystem inflammatory syndrome in children and pediatric COVID-19, Nat. Med. 28 (2022) 1050–1062.

[41] E. Ammirati, J.J. Moslehi, Diagnosis and treatment of acute myocarditis: a review, JAMA 329 (2023) 1098–1113.

[42] P. Zimmermann, L.F. Pittet, A. Finn, A.J. Pollard, N. Curtis, Should children be vaccinated against COVID-19? Arch. Dis. Child. 107 (2022), e1.

[43] K. Goddard, K.E. Hanson, N. Lewis, E. Weintraub, B. Fireman, N.P. Klein, Incidence of myocarditis/pericarditis following mRNA COVID-19 vaccination among children and younger adults in the United States, Ann. Intern. Med. 175 (2022) 1169–1771.

[44] B. Wu, S. You, H. Qian, et al., The role of SIRT2 in vascular-related and heart-related diseases: a review, J. Cell. Mol. Med. 25 (2021) 6470–6478.

[45] X. Tang, X.-F. Chen, N.-Y. Wang, et al., SIRT2 acts as a Cardioprotective deacetylase in pathological cardiac hypertrophy, Circulation 136 (2017) 2051–2067.

[46] H. Morimoto, M. Hirose, M. Takahashi, et al., MCP-1 induces cardioprotection against ischaemia/reperfusion injury: role of reactive oxygen species, Cardiovasc. Res. 78 (2008) 554–562.

[47] H. Morimoto, M. Takahashi, A. Izawa, et al., Cardiac overexpression of monocyte chemoattractant protein-1 in transgenic mice prevents cardiac dysfunction and remodeling after myocardial infarction, Circ. Res. 99 (2006) 891–899.

[48] P.M. Martinelli, E.R.S. Camargos, G. Morel, C.A.P. Tavares, P.R.A. Nagib, C.R. S. Machado, Rat heart GDNF: effect of chemical sympathectomy, Histochem. Cell Biol. 118 (2002) 337–343.

[49] R.H. Baloh, H. Enomoto, E.M. Johnson, J. Milbrandt, The GDNF family ligands and receptors - implications for neural development, Curr. Opin. Neurobiol. 10 (2000) 103–110.

[50] K.V. Dergilev, I.B. Beloglazova, Z.I. Tsokolaeva, Y.D. Vasilets, E.V. Parfenova, Deficiency of Urokinase-type plasminogen activator receptor is associated with the development of perivascular fibrosis in mouse heart, Bull. Exp. Biol. Med. 173 (2022) 5–9.

[51] A. Xiong, L. Duan, J. Chen, et al., Flt3L combined with rapamycin promotes cardiac allograft tolerance by inducing regulatory dendritic cells and allograft autophagy in mice, PLoS One 7 (2012), e46230.

[52] J.S. Bednash, F. Johns, N. Patel, T.R. Smail, J.D. Londino, R.K. Mallampalli, The deubiquitinase STAMBP modulates cytokine secretion through the NLRP3 inflammasome, Cell. Signal. 79 (2021), 109859.

[53] S. Toldo, E. Mezzaroma, A.G. Mauro, F. Salloum, B.W. Van Tassell, A. Abbate, The inflammasome in myocardial injury and cardiac remodeling, Antioxid. Redox Signal. 22 (2015) 1146–1161.

[54] S. Toldo, A. Abbate, The NLRP3 inflammasome in acute myocardial infarction, Nat. Rev. Cardiol. 15 (2018) 203–214.

[55] Y. Zhao, M. Wang, Y. Li, W. Dong, Andrographolide attenuates viral myocarditis through interactions with the IL-10/STAT3 and P13K/AKT/NF-κβ signaling pathways, Exp Ther Med 16 (2018) 2138–2143.

[56] B. Wei, Y. Deng, Y. Huang, X. Gao, W. Wu, IL-10-producing B cells attenuate cardiac inflammation by regulating Th1 and Th17 cells in acute viral myocarditis induced by coxsackie virus B3, Life Sci. 235 (2019), 116838.

[57] A.P. Hutchins, D. Diez, D. Miranda-Saavedra, The IL-10/STAT3-mediated anti-inflammatory response: recent developments and future challenges, Brief Funct Genomics 12 (2013) 489–498.

[58] C.N. Gruber, R.S. Patel, R. Trachtman, et al., Mapping systemic inflammation and antibody responses in multisystem inflammatory syndrome in children (MIS-C), Cell 183 (2020) 982–995.e14.

[59] E.K. Koltsova, K. Ley, The mysterious ways of the chemokine CXCL5, Immunity 33 (2010) 7–9.

[60] X. Fan, C.T. Ng, D. Guo, et al., Dampened inflammation and improved survival after CXCL5 Administration in Murine Lupus via myeloid and neutrophil pathways, Arthritis Rheum. 75 (2023) 553–566.

[61] L.M. Yonker, Z. Swank, Y.C. Bartsch, et al., Circulating spike protein detected in post-COVID-19 mRNA vaccine myocarditis, Circulation 147 (2023) 867–876.

[62] J.S. Halsell, J.R. Riddle, J.E. Atwood, et al., Myopericarditis following smallpox vaccination among vaccinia-naive US military personnel, JAMA 289 (2003) 3283–3289.

[63] M.R. Gubbels Bupp, T.N. Jorgensen, Androgen-induced immunosuppression, Front. Immunol. (2018) 9.

[64] Y. Moriyama, H. Yasue, M. Yoshimura, et al., The plasma levels of dehydroepiandrosterone sulfate are decreased in patients with chronic heart failure in proportion to the severity, J. Clin. Endocrinol. Metab. 85 (2000) 1834–1840.

[65] S. Nakamura, M. Yoshimura, M. Nakayama, et al., Possible Association of Heart Failure Status with Synthetic Balance between Aldosterone and Dehydroepiandrosterone in human heart, Circulation 110 (2004) 1787–1793.

[66] R. Straub, A. Schuld, J. Mullington, M. Haack, J. Scholmerich, T. Pollmacher, The endotoxin-induced increase of cytokines is followed by an increase of cortisol relative to dehydroepiandrosterone (DHEA) in healthy male subjects, J. Endocrinol. 175 (2002) 467–474.

[67] A. Mustafa, F. Nyberg, M. Mustafa, et al., Growth hormone stimulates production of interferon-gamma by human peripheral mononuclear cells, Horm. Res. 48 (1997) 11–15.

[68] J. Giron-Gonzalez, F. Moral, J. Elvira, et al., Consistent production of a higher TH1: TH2 cytokine ratio by stimulated T cells in men compared with women, Eur. J. Endocrinol. (2000) 31–36.

[69] S. Frisancho-Kiss, M.J. Coronado, J.A. Frisancho, et al., Gonadectomy of male BALB/c mice increases Tim-3+ alternatively activated M2 macrophages, Tim-3+ T cells, Th2 cells and Treg in the heart during acute coxsackievirus-induced myocarditis, Brain Behav. Immun. 23 (2009) 649–657.

[70] S.A. Huber, B. Pfaeffle, Differential Th1 and Th2 cell responses in male and female BALB/c mice infected with coxsackievirus group B type 3, J. Virol. 68 (1994) 5126–5132.

[71] D.C. Lyden, J. Olszewski, M. Feran, L.P. Job, S.A. Huber, Coxsackievirus B-3-induced myocarditis. Effect of sex steroids on viremia and infectivity of cardiocytes, Am. J. Pathol. 126 (1987) 432–438.

[72] S.A. Huber, Autoimmunity in coxsackievirus B3 induced myocarditis, Autoimmunity 39 (2006) 55–61.

[73] A. Barmada, J. Klein, A. Ramaswamy, et al., Cytokinopathy with aberrant cytotoxic lymphocytes and profibrotic myeloid response in SARS-CoV-2 mRNA vaccine-associated myocarditis, Sci Immunol 8 (2023) eadh3455.

[74] H. Patel, A. Sintou, R.A. Chowdhury, et al., Evaluation of autoantibody binding to cardiac tissue in multisystem inflammatory syndrome in children and COVID-19 vaccination-induced myocarditis, JAMA Netw. Open 6 (2023), e2314291.

[75] D. Lee, J. Le Pen, A. Yatim, et al., Inborn errors of OAS-RNase L in SARS-CoV-2-related multisystem inflammatory syndrome in children, Science 379 (2023) eabo3627.